European Commission

JRC TECHNICAL REPORTS

Data Analysis of Non-standard Time Series

The role of graph Laplacians and covariance matrices in data and processes of complex systems.

E. Gutiérrez, F. Bono, C. Coutsomitros

2016

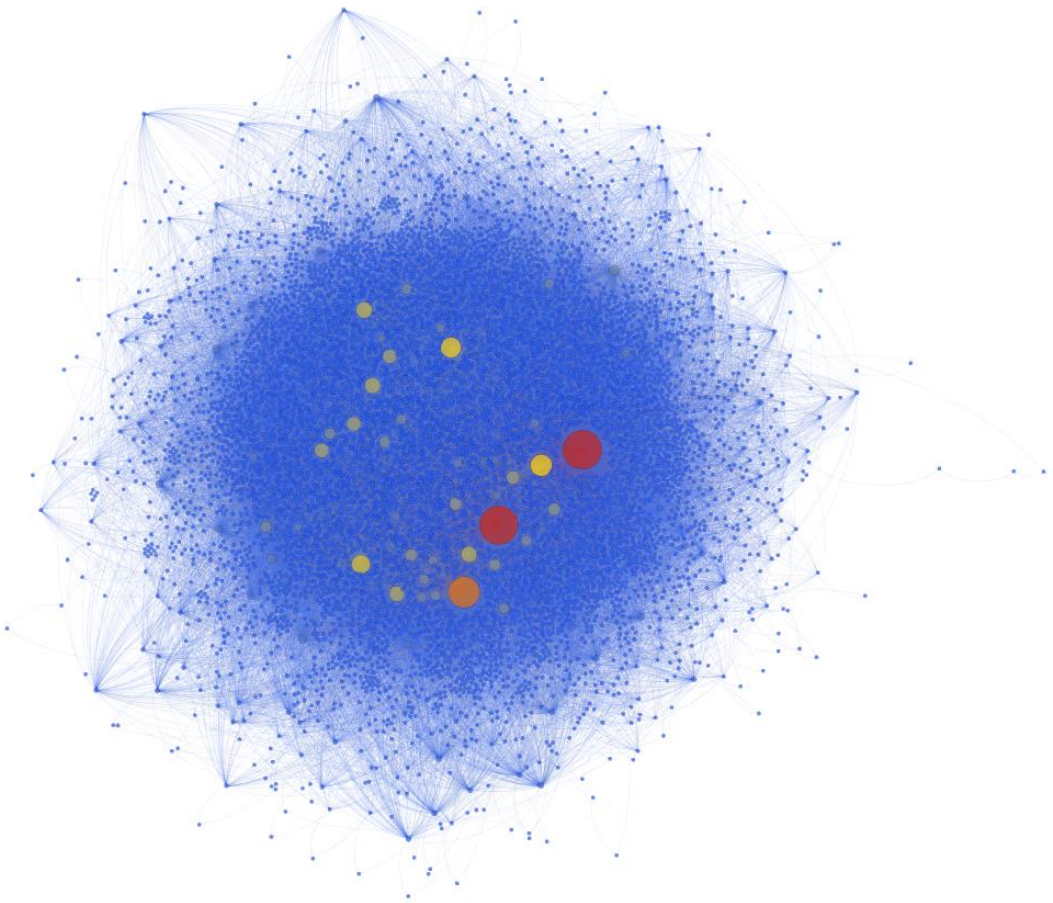

EUR 28191 EN

Joint Research Centre

Contact information
Name: Eugenio Gutiérrez
Address: TP 480, Via E.Fermi, 2749, I-21027 Ispra (VA), ITALY
E-mail: eugenio.gutierrez@jrc.ec.europa.eu
Tel.: +39 0332 785711

JRC Science Hub
https://ec.europa.eu/jrc

JRC103730

EUR 28191 EN

PDF	ISBN 978-92-79-63458-1	ISSN 1831-9294	doi:10.2788/1139
Print	ISBN 978-92-79-63459-8	ISSN 1018-5593	doi:10.2788/657170

Luxembourg: Publications Office of the European Union, 2016

How to cite: E. Gutiérrez, F. Bono, C. Coutsomitros; Data Analysis of Non-standard Time Series: *The role of graph Laplacians and covariance matrices in data and processes and complex systems.*; EUR 28191 EN; doi:10.2788/1139

Deliverable Administration & Summary		WP 852: DYSTECS		CONTAINSTECH	
No & name	D3 2016 **Data Analysis of Non-standard Time Series**, The role of graph Laplacians and covariance matrices in data and processes of complex systems				
Status	FINAL	Due	15/12/16	Date	4/11/16
Author(s)	E. Gutiérrez, F. Bono, C. Coutsomitros				

Contents

List of Figures

SUMMARY

In this report we provide an informal mathematical introduction to the use of some methods from graph theory for the data analysis of *non-standard* time series. By this we mean information from a channel that is not presented to us in the usual format as a regular sequence of numbers. In particular we are interested in the role of the Laplacian matrix operator in helping us to understand the underlying structure and meaning of information generated from a wide range of sources.

Before introducing any mathematical methods, we provide a synopsis as to some of the concepts associated with complex networks that generate such *non-standard* data, hoping to set the background and motivation for the purpose of our work, namely the practical application of spectral graph analysis.

Although we do not purport to present any new mathematical results we believe that we introduce two aspects of some novelty and value: in the first instance we present an alternative algebraic description of the Dirichlet sum over a graph which we have, serendipitously, discovered to be useful for interpreting spectral bounds of the Laplacian; on another theme we present a simple proof concerning the connection between the Laplacian of physical processes and covariance-based multivariate analysis.

In order to demonstrate the versatility of the Laplacian matrix as a tool to understand complex networks, we provide some of our own examples based on data from written language, computer science and earthquake engineering.

BACKGROUND

This note is meant to invite—and perhaps satisfy—curiosity from those who have heard about the nature of complex networks but were perhaps put off by the conviction that it required a high degree of mathematical skill and technical knowledge. It is true that, at times, to fully appreciate the meaning of some scientific concepts requires a rigorous approach (which we don't pretend to apply here); however, the range of applications of complex networks reminds me of the opening lines by Erwin Schrödinger in his treatise on the interpretation of life in biological systems (1), a field for which he claimed no expertise. His argument was that he would not dispense to engage in a subject so intriguing just because he could not present it as an expert; indeed he claimed that scientific knowledge, being by then so vast, any specialist in one field became a layman when working on some unifying description of the whole. Admittedly, he was one of the greatest intellects of humankind, but

technically we find ourselves in the same condition—if not quite in the same intellectual bracket—in the sense that complex networks cover a vast range of scientific and social fields.

The consolidated interest in the study of complex network systems over the past twenty years or so has resulted in a growing tendency for interdisciplinary collaboration. The thread linking the various fields of this branch of complexity science is that even if the underlying physical phenomena can be disparate, their qualitative manifestations and their mathematical representations are analogous. This apparent transferability of behaviour has resulted in a tendency to use common mathematical methods, motivating further collaboration in mathematics, engineering, and the natural, physical, and social sciences.

Complex networks exhibit special traits that make them stand out from other, shall we say, more predictable ones. Complexity presents itself in many forms, describing widely differing qualitative, but analogously quantifiable, behaviour such as emergence (2) (3), self-organized criticality (4), synergetics (5), synchronization (6), etc., which in turn can be associated to an even wider variety of physical processes ranging from the formation of leopard's spots, the synchronization of fireflies, the intermittent nature of earthquakes (7) or human language, as revealed in the word network of a famous novel shown in Figure 1 .

Complexity does not necessarily arise from complicated systems: A car is complicated but is designed—human factors aside—to produce a predictable, 'simple', response for a given range of inputs. Complexity may arise from relatively simple laws but whose systemic long-term behaviour (meaning in an arbitrary, scale-independent, sense) is difficult to predict.

Complex network analysis, as do most of the applied sciences, borrows from a wide range of mathematical methods. We shall briefly go over some now.

G*raph theory* provides a formal framework to label the relations of systems made up of numerous (sometimes heterogeneous) components. *Statistical* and *Topological* measures allow us to condense certain, often scale-invariant, global properties which come in handy when the network is large and joined up in a non-trivial fashion. *Algebra and algebraic* structures provide a complementary alternative to graph theory and allow us to represent networks in a matrix form, which, by analysing their spectra, provide further insight into a network's internal connectivity and border properties.

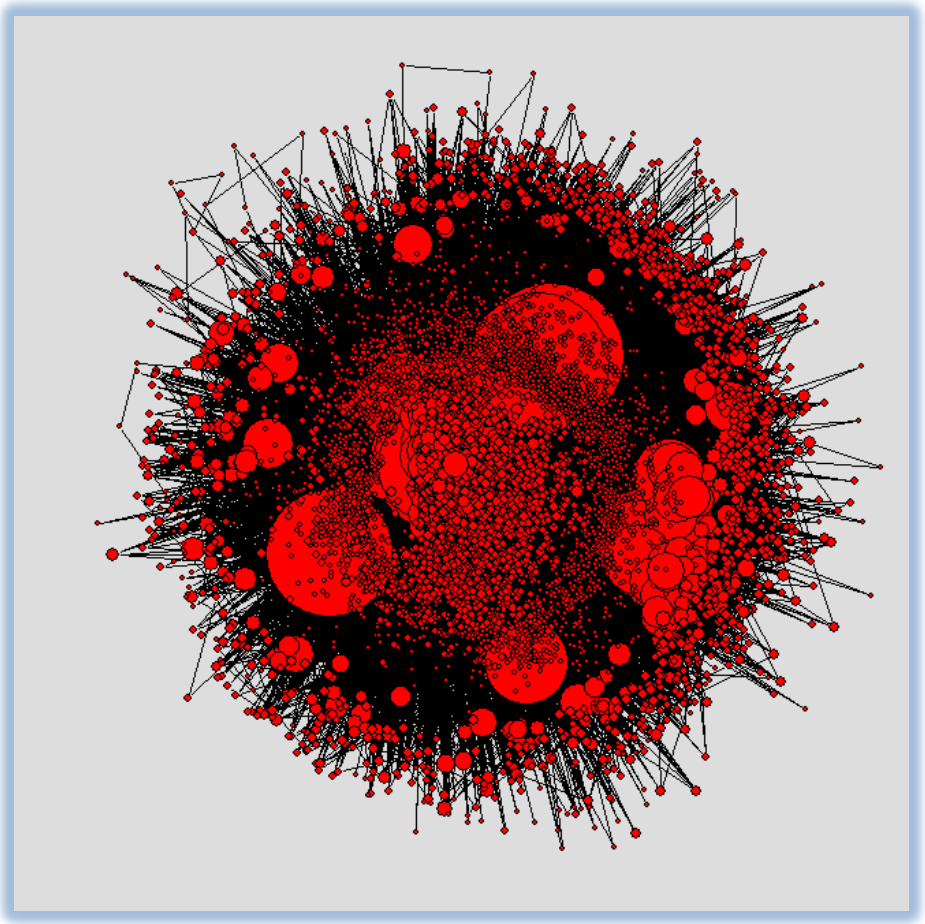

Figure 1 - Complex networks are usually associated with many interacting agents.

The network above consists of over 200-thousand nodes compiled by converting a long string of words into a network adjacency matrix (we will discuss this below). The diameter of the nodes has been exponentially scaled so that their size is related to their weighted degree connectivity. The network is fully connected (no isolates) and consists of so many links that it is difficult to see what is going on. How much can we find out about it with a limited set of mathematical methods?

Dynamical systems theory, be it applied to discrete or continuous systems provides a means to describe the evolution in time and/or space of non-linear processes; such theories can help us to qualify and quantify phenomena such as stability, predictability limits, bifurcations (*aka* catastrophe theory), control, synchronization and *emergence* .

These mathematical methods allow us to study the behaviour of complex networked systems, but what are the common ingredients that make these disparate systems produce such comparable behaviour? There are three that stand out:

- A multitude of interconnected components.
- Non-linear interactions between components.
- Feedback (or equivalently dissipation, hysteresis, delay, memory…).

Having only one characteristic may not be enough to generate, so-called, complex behaviour.

It is true that if the system is composed of just one non-linear element (with or without feedback) it is capable of exhibiting very unpredictable behaviour, such as high sensitivity to parametric or starting conditions (i.e. chaos). Said sensitivity is a major component of complex systems, but that's not all.

If, on the other hand, a system is composed of many linear (or linearized) elements (with or without dissipation) the behaviour will be predictable—stable or otherwise—but not complex. To generate complexity we need something that makes the system behave in manner than is not immediately obvious just by looking at the behaviour of the individual constituent elements that make it up.

The third element in our list is perhaps the most subtle yet it is the most ubiquitous as it crops up in all macroscopic natural phenomena. In some fields it is referred to as feedback, by others as hysteresis (mechanical, magnetic, financial…) or dissipation. It results from a non-recoverable process or mechanism whereby energy is either extracted or introduced into the system in such a manner that the system re-organizes into a form or behaviour that cannot recover unequivocally to its native form: it leaves a *memory* or *path-dependency* of the process. From a mathematical point of view feedback introduces infinite dimensionality into the differential equations of the system, for which no closed-form solutions exist.

If a system combines the elements described above, the full range of attracting states (i.e. the type of data we sample from the system we are monitoring) is characterised by many types of qualitative behaviour which appear and disappear as a consequence of variations of parametric or starting conditions. Such transitions may be observed in a bifurcation diagram from which can identify how simple attracting—periodic or fixed—states cascade and multiply until they transition into, so-called, strange attractors (see Figure 2).

When dealing with the practicalities of modelling or controlling systems that exhibit delay or dissipation, it is usual to make the mathematics more tractable, for example by linearization (or extrapolation in time).

A good example in engineering is linear viscous damping, a purely mathematical concept that does not exist in reality; but when the real physical damping is small enough, one can get away with the linear model approximation. If the system is very non-linear and particularly complicated, recourse to computational methods such as finite difference or finite elements allow us to compute numerically tractable approximations to obtain a solution. Nevertheless, such solutions are, ultimately, numerical experiments, so we are still left with the problem of extracting the core meaning from a sometimes fathomless ocean of data. We could run numerical tests for any number of scenarios but without a unifying qualitative, phenomenological understanding, such 'experiments' may not necessarily explain the intrinsic nature of a complex data set.

Summarising, complex networks are composed of many (but not necessarily identical) components acted on by a non-linear vector field, which *repels* (respectively coalesces) the individual components towards some common state or *phase*, which, depending on certain factors, may be more or less stable and hence resilient to perturbations. In addition to this, other mechanisms introduce memory (hysteresis, feedback, dissipation etc.) that provide a delayed—conversely, anticipated—component of the system's state back into itself, which, in turn, tends to excite or damp down the instantaneous dynamic response. These essential components are sometimes enough to create the extraordinary range of behaviour we see in complex phenomena.

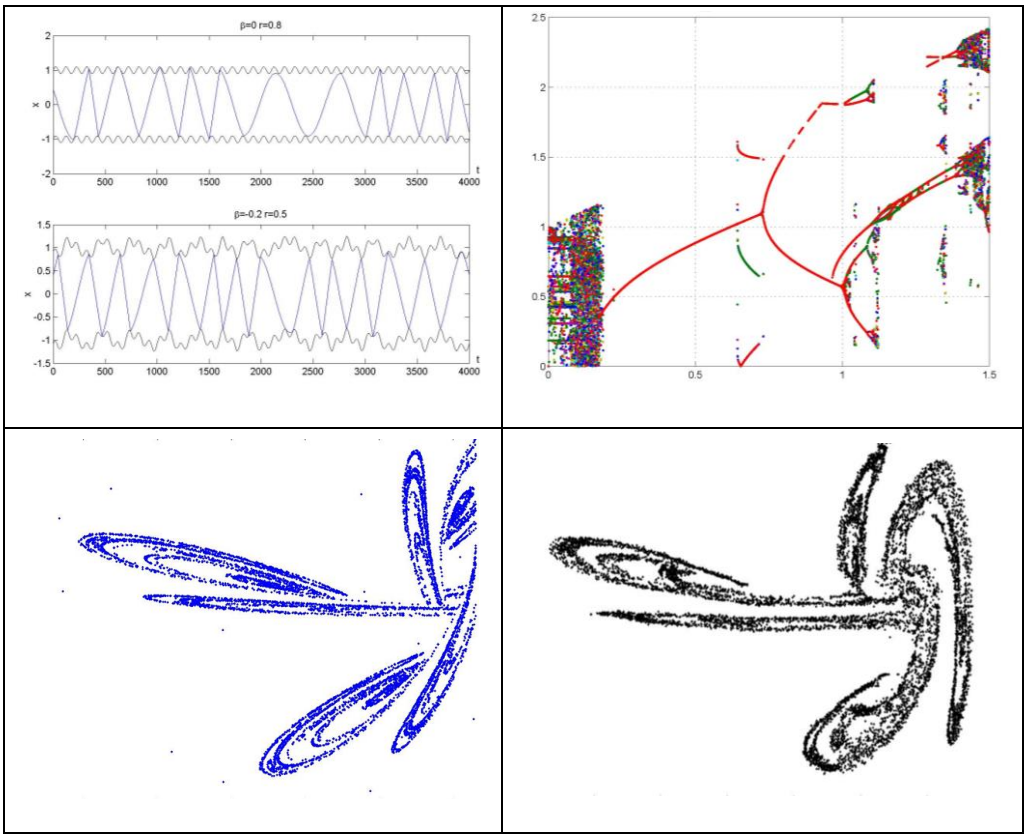

Figure 2 - What does the behaviour of a chaotic system look like?

A, so-called, *strange* attractor is a stable—but very complex—orbit made up of (many, sometimes 'infinitely many') unstable periodic orbits that separate and re-join within some bounded phase space. We can observe this process through a Poincaré section (in this case a stroboscopic 'illumination' at time intervals given by period of the forcing function of the the motion).

Transitions to chaos and strange attractors (top row) : Non-linear mechanical vibrations may become progressively more erratic (top left). In the bifurcation diagrams (top right), as a mechanical factor is varied along the x-axis, the system will suddenly switch, or bifurcate, from simple to multiple periodicity and, eventually, to chaotic states (seen as concatenated branching leading to the fuzzy areas at either end of the x-axis).

In the lower two frames we show numerical (blue, left) and experimental (black, right) versions of a strange attractor produced by a simple spring-mass system. Whereas the real mechanical oscillator is made up of an Avogadro-sized number of atoms, the numerical model consists of just one spring-mass governed by simple rules (Newton's inertial laws of motion and impact restitution, and Hook's spring law), yet the numerical and experimental data look very much alike. This exemplifies two essential characteristics of complex dissipative behaviour; in the first place the tendency of dissipation to exponentially diminish the presence of oscillation modes that are not excited by the driving vector field (condensation of degrees of freedom); secondly, the universality and scale-free nature of the underlying process is such that the physical and numerical oscillators are, in the Newtonian mechanical reference scale, similar; i.e. the same behaviour would be obtained for an oscillator at any scale (see (8)).

Original text:

PART One CHAPTER One
On an exceptionally hot evening early in July a young man came out of the garret in which he lodged in S. Place and walked slowly, as though in hesitation, towards K. bridge.
He had successfully avoided meeting his landlady on the staircase. His garret was….

Atonal unpunctuated text:

part one chapter one on an exceptionally hot evening early in july a young man came out of the garret in which he lodged in s place and walked slowly as though in hesitation towards k bridge he had successfully avoided meeting his landlady on the staircase his garret was ……

Word identifier sequence:

{1 2 3 2 4 5 6 7 8 9 10 11 12 13 14 15 16
17 18 19 10 20 21 22 10 23 24 25 26 27 28 29 10
30 31 32 33 21 34 35 36 37 38 39 4 18 40 38 19
41….}

Edge Sequence:

1	2
2	3
3	2
…	…
…	…
40	38
38	19
19	41
41	…
…	…

Constructing the graph connectivity

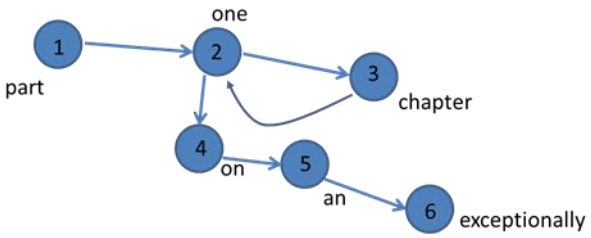

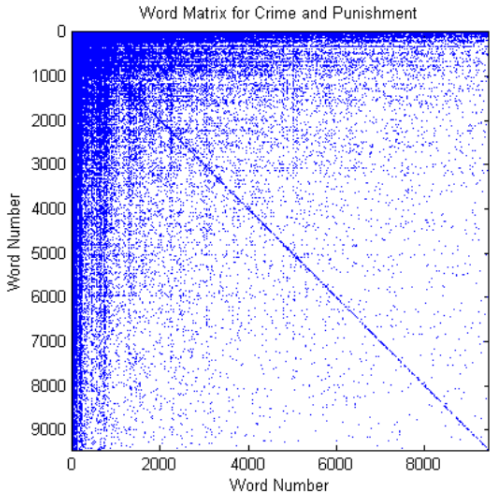

Figure 3 - Language: the ultimate complex network?

Top frame: The opening words to *Crime and Punishment* by Fydor Dostoyevski, followed by atonal text (no punctuation, no inflections). Middle frame: Words are tallied to a number identifier in order of appearance: 'part' **is identified as word 1,** *'one'* **is identified as word 2,** *'chapter'* **is word 3,** *'one'* **reappears again and tallied as the second occurrence of word 2.**

Lower frame: Continuing the process for the whole text we can construct the full adjacency matrix. The weighted connectivity matrix is highly asymmetric (path dependency), reflecting the nature of language itself. The asymmetry in the word-matrix arises from the hysteretic nature of word use: logic, grammar and fashion preclude or enforce certain word orders.

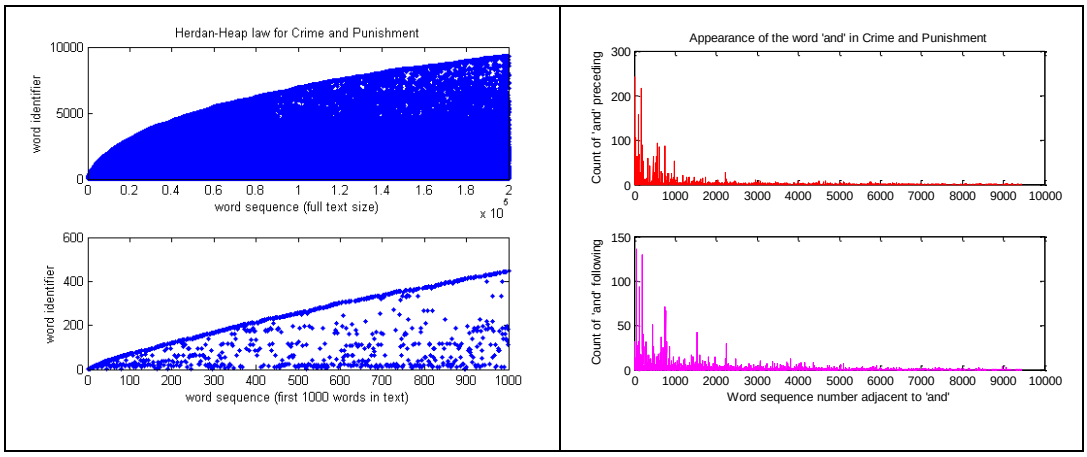

Figure 4 - The Herdan-Heap law predicts that the chances of finding a new word in a body of text diminish as a power law.

Dostoyevski's wrought psychological analysis makes use of about 9500 individual words out of 204-thousand in total (top left); however, of the first 1000 words 500 are new (bottom left). Language hysteresis: Word order and inflection are essential for generating nuanced meanings as shown by the word *'and'* (top right), of which the most common co-occurrence is with word number 18 corresponding to *'the'* (e.g. *'and the'* appears 242 times, but never appears as *'the and'*). For the transpose distribution of *'and'* (lower right), the most common occurrence is with *'him'*, so that *'him and'* appears 136 times, whereas *'and him'* appears only twice.

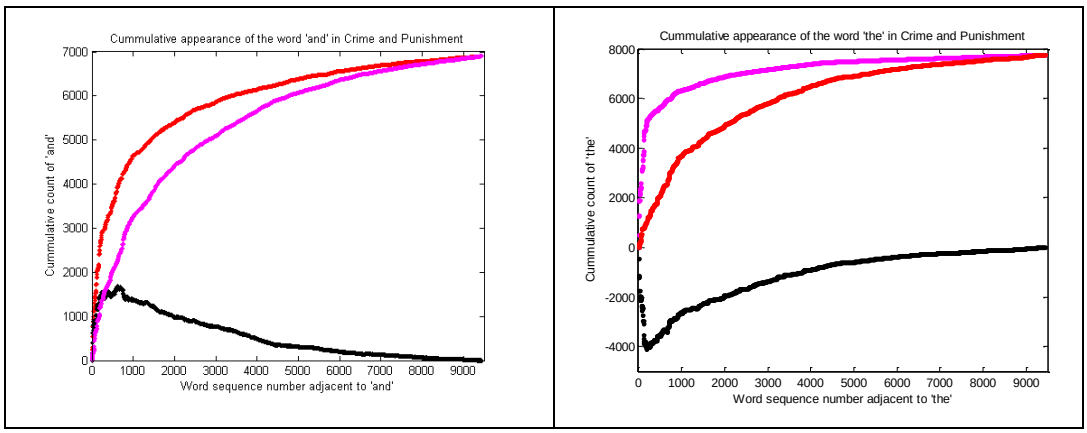

Figure 5 - The total cumulative, appearance and hysteresis of *'and'* and *'the'*.

The difference between the preceding and following word order curves (respectively red and magenta), is highly hysteretic (shown in black). The hysteresis curve peaks early in the text because the most commonly used words associated with *'and'* also appear early on (as expected from the Herdan-Heap law). In contrast, the hysteresis of *'the'* is markedly greater and of different sign to *'and'*, in spite of having similar total occurrence rates (of the order of 8000 times). Given that one is a *conjunction* and the other a *definite article* it would be worthwhile to explore how hysteresis varies with grammatical structure.

We have described the make-up of complex networked systems and provided some examples, now it is appropriate to say something about some of the mathematical developments that are often used in order to understand and explain their behaviour.

In addition to the fundamental theorems and conjectures in dynamical systems, graph theory and topology that—sometimes only much later—were associated with the disparate scientific fields grouped under the umbrella of complex systems, it is fair to say that there is no special unique mathematical method that has been developed to understand complex systems; indeed some mathematicians are of the opinion that there is no new complex systems maths at all, just established mathematical methods applied to a different way of looking at non-linear dynamical systems and complexity. Most of the basics of complexity theory were formulated over a century ago and most of the newer, more exotic-sounding terms in the complexity lexicon, such as chaos, self-organised systems, fractals etc., were coined a decade either side of the seventies.

Nevertheless, it is perhaps worth reminding ourselves of two original perspectives of how chaos/complexity theory came about, and, in passing, we suggest reading the *scholarpedia* web-page by Phillip Holmes[1] and his paper (9) on the subject. From our own personal choice we must point out two pivot concepts.

(i) The insight of Henri Poincaré who, over a century ago, by showing how a deterministic physical system can generate unpredictable and wildly oscillating phenomena, laid down the basis for both analytical and future, computer-generated, numerical investigations into dynamical systems that hitherto had had to be restricted to linear, linearized, or mathematically tractable formulations.

(ii) The developments in topology and graph theory, initiated by Euler in the 18th century, were complemented in the 20th by the introduction of probabilistic methods following the seminal work of Paul Erdős on random graphs. In turn, this motivated the development of methods based on spectral graph theory, statistical and time series analysis which, allied to the vast increase in

[1] http://www.scholarpedia.org/article/History_of_dynamical_systems

computational power, led to the development of applied complex network analysis to real-world cases (10) (11) (12).

In order to uncover the underlying structure of both experimental and computer-generated data of complex systems, a wealth of numerical methods, grounded in the key concepts described above, have been adapted to develop a suite of time-series analysis procedures and software packages, specifically geared to be applied to data structures that are known to exhibit chaotic or complex behaviour (see for example Abarbanel in (13)). We remind, again, that most of these techniques are not particularly recent, but rather they are used with the presence of mind as to their subject. Thus, for example, when a Fast Fourier Transform is applied to the time series of a chaotic attractor, the appearance of a flat or undifferentiated spectrum is not to be ascribed to 'noise'; nor that a spectrum with three discrete peaks implies the system has three degrees of freedom. Likewise, methods borrowed from information, control theory and topology such as average mutual information, Lyapunov stability and point set dimensionality require that the user appreciates that the standard signal diagnostics may not apply to complex systems.

Notwithstanding the importance of the methods glossed over in the preceding paragraph, in this manuscript we have chosen to highlight the importance of the role that algebraic structures of complex networks, and in particular the Laplacian matrix, play for both describing and understanding the fundamental nature of interconnected systems. Clearly, the Laplacian matrix is not new to mathematics; however, what has garnered much interest over the last two decades or so, is its transition from a specialist topic of graph theory into real-world applications, ranging from pattern recognition (14) to engineering systems (15) and quantum computation (16).

Although we do so in an informal manner we will strive to provide the basic mathematical formulations, barely hinting at the full range of the Laplacian's properties. For a formal and more error-free description, we leave the reader to consult the few, but highly authoritative references we have provided in the bibliography on this topic. First we shall state the basic definitions for graph structures, from where we define the Laplacian and some of its basic spectral properties. Subsequently we will describe some applications in engineering, computer science, and multivariate analysis, wrapping up with some important pointers to how the Laplacian is linked to other fundamental theorems from other fields of mathematics.

CONCEPTS:

GRAPH THEORY BASICS

In the preceding sections we have already provided intuitive concepts concerning graph constructs and terminology. The following is a quick résumé of some basic graph-theoretic terms.

Given an undirected graph $\mathrm{G} = (\mathrm{V}, E)$ defined by the vertex set

$\mathrm{V} = \{v_1, v_2 \ldots v_n\}$, the edge set $E = \{e_1, e_2 \ldots e_n\} \subset V \times V \;\; C(E)$.

Remembering that the degree, *d*, of a node *i* is the number of nodes connected to it. So a vertex with degree 0 is an isolate and a vertex with degree 1 is an end-vertex. A graph may be made up of an arbitrary ensemble of disconnected or connected vertices (i.e. of arbitrary degree *d*). The order of G is the cardinality of its vertex set and the size, or volume, of G is the cardinality of its edge set, i.e. $\mathrm{vol}\, G = \sum_{i \in G} d_i$.

Graph spectral analysis is concerned with the Eigenproblem associated with certain matrix representations of graphs. Graph spectra approaches have applications in understanding inherent characteristics of graphs, ranging from random walks to partitioning (17); in this paper we wish to examine how the spectra of G are connected with physical phenomena when we assign a functional or phenomenological meaning (physical, social, linguistic..) to the nodes and edges.

ADJACENCY AND LAPLACIAN

The adjacency, or connectivity, matrix, A, of the graph G is given by the *n*x*n* matrix with elements

(1) $$A_{i,j} = \begin{cases} 1 \text{ if } i, j \text{ are connected} \\ 0 \;\; \text{otherwise} \end{cases}$$

Next we define the degree matrix which is given by

(2) $$D_{jj} = \sum_{i=1}^{n} A_{i,j},$$

which is diagonal and indicates the degree of each node. The next step is to generate the matrix formed from the difference between the degree matrix and the adjacency matrix; this is called the Laplacian matrix of a graph and is given by

(3) $$L = D - A.$$

At this stage we should say something about how the eigenvalues of L are associated with graph connectivity before we return to this issue in greater depth later. For the case of symmetric adjacency matrix A, L is positive semi-definite, so that its eigenvalues $\lambda_{i=0:n-1}$ are positive real and at least the first must be equal to zero (18) (19) (17) (20) (21) (22). So we have that

(4) $$0 = \lambda_0 \leq \lambda_1 \ldots \lambda_{n-1}.$$

If only the first eigenvalue is zero then all the nodes of the graph are connected so that there is at least one path from each node to every other. If we find that there is more than one zero eigenvalue then there is more than one single connected component. The values and distribution of the eigenvalues of the individual components can tell us more about their connectivity, size and order, and of these we are particularly interested in the first non-zero eigenvalue, λ_1, often referred to as the *Fiedler* value (23). The Fiedler value results from some well-known results in linear algebra; it crops up in many mathematical problems and has many implications for applications in science and engineering. The Fiedler eigenvalue may be obtained by selecting it from the complete eigenproblem or through numerical iteration via the *Rayleigh Ratio* and the *Courant Fischer* expression (Appendices A, B)

THE NORMALISED LAPLACIAN

The Laplacian can be normalised by certain diagonal matrices, some of which, as we shall show below, are very familiar in engineering applications.

Let's start off with the most common formulation for the normalised Laplacian matrix based on the degree matrix D as described in (17) in Appendix C. We define the normalised Laplacian as

(5) $$\mathbf{L}_{i,j} = \begin{cases} 1 \text{ if } i = j \text{ and } d_i \neq 0 \\ -\dfrac{1}{\sqrt{d_i d_j}} \text{ if i and } j \text{ are adjacent,} \\ 0 \text{ otherwise} \end{cases}$$

which is equivalent to

(6) $$\mathbf{L} = D^{-1/2} L D^{-1/2},$$

The normalised Laplacian has a notable array of properties (17) (19) (21) and is so ubiquitous that a number of fields given it special names solely associated to their field of science (i.e. stiffness, Kirchhoff, matrices etc.). We also remark that the related product

(7) $$\tilde{\mathbf{L}} = D^{-1} L$$

is co-spectral (i.e. has same spectral signature) as $\mathbf{L}$, but whereas $\mathbf{L}$ is symmetric, $\tilde{\mathbf{L}}$ is not necessarily so; this results in differing eigenvector sets. We shall revisit this issue considering the mass orthonormalisation in structural systems.

It is worth pointing out at this stage that the graph Laplacian is the discrete equivalent of the Laplacian operator, and, moreover, that the Fiedler eigenvalue for a graph corresponds to the eigenvalue of the Laplace-Beltrami operator for non-Euclidian surfaces (17). We shall return briefly to this connection later on when we discuss isoperimetric problems and graph tomography.

LAPLACIANS IN ACTION

AN EXAMPLE FROM MECHANICS

The formulation of the Laplacian can be used as a simple means of generating the stiffness matrices of discrete systems (for a more extensive overview applied to engineering systems see (15), and for a similar approach with a more generic application in the inverse sense; i.e., of evaluating the structure from the Laplacian see Section 9.2 of (5))

Consider the case of a simple three-degree-of-freedom spring–mass system below.

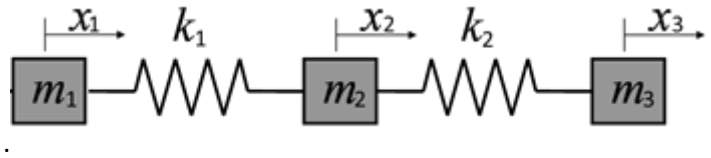

Figure 6 - A spring-mass system.

For the sake of simplicity we assign the springs stiffness $k_1=k_2=1$ as the edges, and the nodes to the mases m_1,m_2,m_3. First we construct A, D *and* L as follows

(8) $$A=\begin{bmatrix}0&1&0\\1&0&1\\0&1&0\end{bmatrix};D=\begin{bmatrix}1&0&0\\0&2&0\\0&0&1\end{bmatrix};L=\begin{bmatrix}1&-1&0\\-1&2&-1\\0&-1&1\end{bmatrix};$$

From where we see that L is identical to the stiffness matrix arrived at through the stiffness or flexibility method. The meaning of the spectral modes is such that the first eigenvalues, $\lambda_0 = 0$, corresponds to the rigid-body translation of the system with no spring distortion, whereas the first non-zero eigenvalue, λ_1 (the Fiedler value), is simply the first-mode (or natural) vibration extension mode. The effective natural dynamic vibration modes will depend on the value of the masses. If we use the diagonal mass matrix M instead of the degree matrix D, where

(9) $$M=\begin{bmatrix}m_1&0&0\\0&m_2&0\\0&0&m_3\end{bmatrix}.$$

The mass-orthonormalised Laplacian is

(10) $$\tilde{\mathbf{L}} = M^{-1}L$$

The eigenvalues so obtained now correspond to the natural vibration modes of the spring-mass structure, and the eigenvectors of $\tilde{\mathbf{L}}$ are simply the mass-orthonormalised modes of those obtained from $\mathbf{L}$.

The Laplacian matrix shown here is given for the unweighted case where the connections between masses are either 1 or 0. However, Laplacians can also be constructed for cases where the connections are weighted, i.e. where some connections are stronger/stiffer than others, or not symmetric (for example, a bi-directional spring). We shall return to this issue when we examine heuristically-generated *asymmetric Laplacians* later on.

An example of a weighted matrix approach is shown in (24) and (25) to evaluate the modal participation factors in the European High voltage electricity grid system by equating power line capacities to the weighted links and the power stations and major transformer sites as nodes. By summing the participation factors along all paths it is possible to identify congested power corridors that are more prone to overloading. Again, just to draw analogies, such modal combination rules are used in earthquake engineering design of structures (26)

We've all heard of the expression *the weakest link in the chain*; in mathematical terms we could say the *Fiedler link of the chain*. We noted that the Laplacian of a connected graph (i.e. one with no dangling nodes) has exactly one eigenvalue equal to zero, and, indeed, that the cardinality of eigenvalues equal to zero corresponds to the number of connected components. It follows, then, that if we want to see how close a connected system is to breaking up, how vulnerable (or alternatively resilient) it is, or how much effort we need to reconnect it again, then all we need to do is keep an eye on the Fiedler eigenvalue(s) in relation to the full graph spectrum. More specifically, we might want to perturb some parameter (perhaps eliminating or modifying the value of certain link or links) and monitor if the Fiedler value approaches zero.

It so happens that this problem is associated (actually, it's the inverse) of another, far older, one: the *isoperimetric* problem concerning the closed curve of a given perimeter that encloses the greatest area. In our case we could ask, what is the shortest cut that will divide an area into two nearly equal ones? In graph terms the question would be which set of links will split a given network into two large components? Such a set of links make the network vulnerable. If one wants to incapacitate a network (conversely rebuild or protect it) then one searches for this set.

When a network has a simple topology (connectivity), identification of the vulnerability links is straightforward. Consider a chain of identical links; it is clear that taking out the middle one is the best cut to divide the chain in two smaller ones of equal size. But what happens if the network is large and complex? Solving for the Fiedler problem of the normalised Laplacian will provide an answer but it may be computationally expensive to solve the complete eigen-problem; however, in some cases we needn't have to do so. One can solve for the first few eigenvalues taking the approach shown in Appendix B and exploit the Courant-Fischer property and Raleigh quotient to iterate quickly to the lowest (or highest) eigenvector eigenvalue pair using, for example, the Lanczos algorithm (19).

Let's follow this up with a more intuitive example. We stated earlier that the Courant-Fischer form for the Fiedler value is analogous to the eigenvalue of the Laplace-Beltrami (LB) operator for Riemannian manifolds (Appendix C). In analogy to bisecting discrete graphs, the eigenvalue of the LB operator can be used to identify the best perimeter bisection path on non-Euclidian surfaces.

For example, consider a non-Euclidian manifold such as the husk of *a peanut* which is composed of both hyperbolic and elliptic manifold surface sections; intuition suggests that the perimeter around the pinched section is what we are looking for when we look for the optimum cut. The eigenvalues of the LB operator should point to that section (see Figure 7).

We have discussed how the Fiedler eigenvalue plays a role in identifying the nodes where possible sectioning is optimized. Now, if we wish to identify those nodes that lie on the steepest ascent along the Fiedler Eigenvector, ψ_{λ_1}, we can calculate the neighbourhood gradient around each node. We recall, in simple terms, that the gradient for a one-dimensional data field is simply the derivative, and, if the data are discretely sampled (for instance, a time series) then the discrete derivative, to a first approximation, is simply the difference between two successive points. We remark that, in essence, two successive points are simply two neighbouring points.

For a diagonal matrix M of the form of (9), that can be any arbitrary function assigned to the nodes, one can chose to assign M as the eigenvector of the Fiedler eigenvalue i.e.

$$M = diag(\psi_{\lambda_1}).$$

We have used this approach and projected the Fiedler eigenvector onto the vertices of the peanut shaped object shown in Figure 7.

In a previous JRC report (27) it was shown how the Fiedler eigenvector of the Laplacian matrix projects onto the optimal cut edge set of a network. An efficient cutting strategy is therefore to select those nodes with the highest modal gradient of the Fiedler vector. In general we can progressively cut the network into smaller and smaller groups by identifying those nodes with the highest gradients of the Fiedler vector with respect to their neighbours.

The next step is how to evaluate this gradient for a generic graph. In the first instance we can associate the concept of neighbourhood derivate on a graph to that of a derivative of a discretely-sampled time series by starting with the following simple example: Make each point in a discretely-sampled time series equivalent to a node in a graph so that the graph has as many nodes as sampled data points.

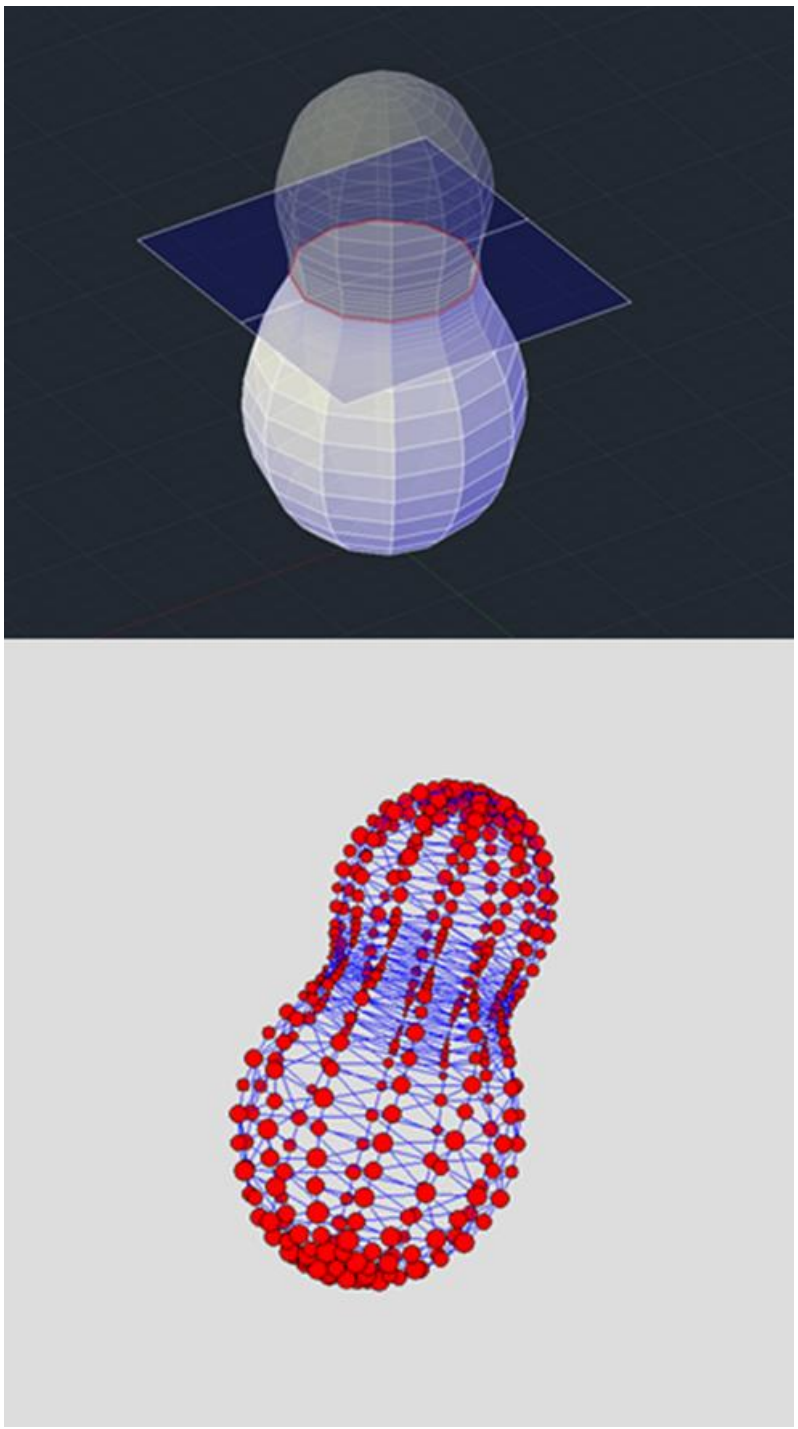

Figure 7 – A plane associated with zeroth transitions of the discreet LB eigenfunction.

Top frame: **the discretized mesh.** ***Lower Frame:*** **The absolute values of the Fiedler eigenvector are assigned to each node; if one looks closely it can be seen that the size of the nodes tends to zero as they approach the pinched section.**

We say that two nodes a_n, a_{n+1} (i.e. two data points) are connected if they proceed or precede each other by one time-step, we represent their connectivity in the graph matrix A as $A_{(n,n+1)}=1$. We now assign to each node (i.e. to each data point) some value of the variable in question (voltage, displacement etc.). This generates the diagonal matrix M. In this one-dimensional form of consecutive points, the edges represent an independent variable such as time, but if we replace time, by distance say, then we can associate topological connectivity with physical proximity in discrete steps. We can generalize the concept of neighbourhood to any dimension for any number of neighbours in a generic way and represent topological neighbourhoods on a graph via the connectivity matrix A.

We now define the gradient of the connectivity matrix A of graph *G* with internode spacing variable δ over the node weight matrix M as.

(11) $$Grad(A,M,\delta)=\left[AM-(A'M)'\right]\times\delta^{-1}.$$

It can be shown that the definition of gradient coincides with the differences in the neighbouring nodal values required to define the *Dirichlet* sum (se Appendix B).

The gradient matrix can be interpreted as follows; the main diagonal is identically zero and represents the gradient of each point to itself. Even for a symmetric matrix A, *Grad* is anti-symmetric[2], thus the first upper diagonal is the discrete derivative forward in time and the first lower, that of reversed time. If A is directed then only paths in the connected direction will appear.

CHEEGER NUMBERS FOR GRAPHS

There is still another connection between the isoperimetric problems and the bounds of the Fiedler eigenvalue. A more extensive description may be found in Appendix E, but in essence it builds on the concept of measuring the minimal number of cuts that produce the maximal bisection for a discrete graph, i.e. the border set ∂S between two subsets S and its complement $\overline{S}$ such that $S\cup\overline{S}=V(G)$. The ratio of the border set to the smallest bisected sets is known as the discrete form of the Cheeger number $h_G(S)$, and the smallest of all possible $h_g(S)$ is known as the Cheeger constant, h_G, of graph G. For the example, suppose we had ten nodes joined by nine links, Figure 8, and we cut the 1st link from one

[2] Implies eigenvalues are complex pairs.

side leaving two components consisting of one isolate and a nine-node chain, then the Cheeger number, h_G (), would be

$$h_G(S\{1\}) = (1\ link\ cut)/(1\ \text{node})=1, \quad (12)$$

as it is the ratio of the number of cuts over size of the smallest bisection. If we cut the chain somewhere towards the end on the other side—link number seven say, then

$$h_G(S\{8,9,10) = (1\ link\ cut)/(3\ \text{nodes})=1/3. \quad (13)$$

The Cheeeger constant for a graph is the smallest of all the h_G (), in this case we obtain the best cut when we eliminate the central link: h_G=1/5.

$$h_G(S\{6,7,8,9,10\}) = (1\ link\ cut)/(5\ \text{node})=1/5 \quad (14)$$

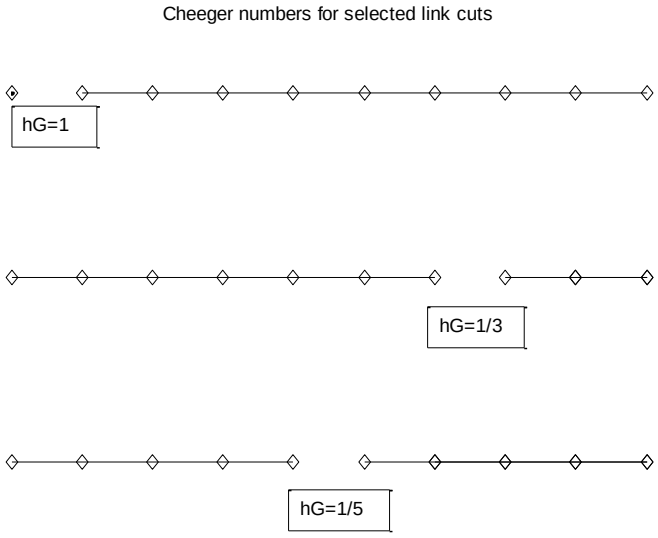

Figure 8 - Cheeger numbers for a nine-link, ten-node {1,2,3…10}, chain graph .

Cheeger numbers, $h_{G()}$ for the graph are shown for some possible cuts. The graph Cheeger number corresponds to the minimum h_G=1/5.

There is an interesting relation between the Cheeger number and the Fiedler value, known as the Cheeger inequality

$$2h_G \geq \lambda_1 \geq \frac{h_G^2}{2}. \quad (15)$$

The implications of the connection between the Cheeger number and the spectra of the Laplacian are far reaching. For a start it provides an alternative, and often computationally cheaper, method of evaluating the bounds of the Fiedler value. There are also a

number of limits and inequalities associated with so-called expander graphs (important for sensor networks deployment and resilience quantification, amongst other things). The approach above can be applied to weighted graphs; so for the example of the chain graph shown in Figure 8, if the middle link is slightly weaker than all the others, the Cheeger number would be even smaller, and hence accentuate the efficiency of the cut. Alternately, a particularly weak link situated towards either end of the chain could derive an even smaller h_G value even if the size of the smaller bisected component is not the largest possible.

If we ascribe some functionality to the chain integrity (suppose it is a simple model for a bridge or some other form of connectivity in an infrastructure network), and assign to each node a functionality or asset value, then the Cheeger number permits the evaluation of simple bounds to assess vulnerability (such as for progressive collapse of a structure).

With due consideration of scale and node-link functionality, such an approach could be applied to other networks, such as, for example, the impact of connectivity and directionality in urban traffic. In (28) it was found that a localised Cheeger-like measure indicated a clear correlation to traffic densities.

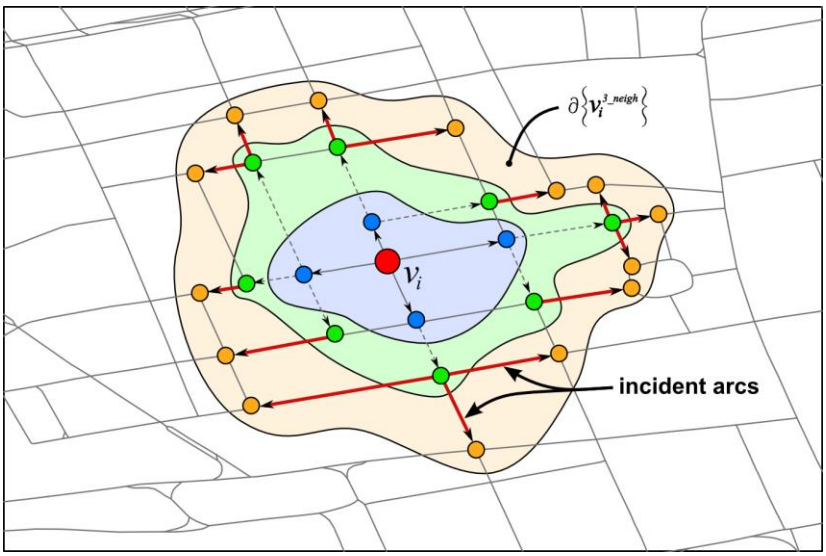

Figure 9 - An example of perimetric measures applied to the urban road network (taken from (28)).

For a given graph distance from a reverence node, a weighted Cheeger-type measure is evaluated and correlated to measured traffic in urban roads. The perimetric measure is then amalgamated and examined as a function of graph distance for the complete urban data set.

In the introductory sections above, we commented on how one of the characteristics of complex systems is the issue of, so-called, emergent properties. *Emergent behaviour* is the ultimate counterexample to the deterministic predictable universe in the sense that, under some circumstances, one can create a deterministic system capable of exhibiting wholly unexpected qualitative behaviour. The best example of this is how the mixing and activation of organic chemical reactions—none of whose molecules are 'alive'— somehow evolve into a living organism. Some authors recently suggested that life emerges from the network dynamics between inanimate molecules (29); in this and other manifestations of biological, ecological and social phenomena (5) the role of the adjacency, and hence the Laplacian, matrix is fundamental to the emergence of other aggregated dynamics such as flocking, traffic jams or crowd behaviour (30) .

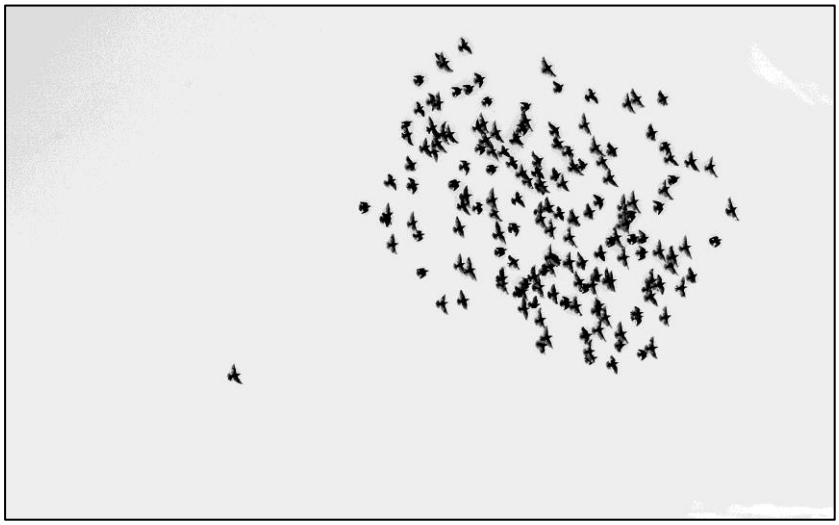

Figure 10 - Birds Flocking.
Even when relative positions between birds change slightly, the flocks move in unison. It is conjectured that even simple rules generate convergence of the flock. The rate of convergence and stability of the murmuration depends on the spectral properties of the Laplacian and the arbitrary rates of separation between flock members.

An interesting application is the study of the emergence of flocking. Are we to presume that birds are capable of developing strategic flocking plans, and, do we also presume that each bird is keeping a watchful eye on every other bird and working out the dynamics of the whole? At the core of a series of papers on the mathematics of emergence, Cucker and Smale (3) (31) prescribed the Laplacian matrix as the central mathematical object used to quantify the process of emergence. They showed how the kinematics of flight based on simple rules of attraction between agents (in this case line-of-site-distance between flying birds) may bring about the

phenomenon of flocking or murmurations. In order to quantify the qualitative concept of emergence the authors point to the evolution of the Fiedler eigenvalue of the Laplacian flight matrix. In essence, a murmuration is formed when all the birds in a flock do something together (in this case fly in a group at similar speed and direction), but the murmuration may change shape and move through 3D space in sometimes very complex patterns. In other words what we are looking for is the emergence of a single connected component (i.e. a single zero eigenvalue) as a function of the visibility parameters and starting conditions of the birds. Although emergence can be defined in an algebraic sense as the spectral evolution of Laplacians, it must be understood, however, that without a mechanistic knowledge of how these rules evolve from biological or ecological constraints we are still left without a driving principle.

Computer Science: Continuous Quantum Walks

Recently, scientists in biology and ecology have discovered that quantum effects are responsible for everyday macroscopic behaviour such as photosynthesis, sight, bird migration and sense of smell (for further sources see (32)); but in the area of computer science quantum mechanics is set to play an even greater role than it has already done in modern electronics, and here, the Laplacian matrix plays a central role.

The Laplacian matrix is so ubiquitous that when scientists familiar with its characteristics by chance encounter it in a discipline far-removed from their own; the initial surprise is often followed by the curiosity as to how it is used in a field of which they have only but a peripheral knowledge. A good example of this is the use of the Laplacian in the field of quantum walks (continuous or discrete) which purport to describe the evolution (expressed in complex probability functions) of a quantum particle traversing a discrete medium such as a lattice or a network. Such a network, at the most basic level, could represent quantum computation architectures. This serves as a basis to develop a means of modelling the effects of quantum entanglement and interference in networks handling quantum bits (Qubits); such networks serve as precursors for quantum computation logic circuits, encryption keys and other areas currently being studied under the general theme of quantum information.

At this level, the underlying physics is governed by quantum mechanics and the quantum walk is deemed to occur on a graph (for example through an optic fibre network). A more extensive, but still

non-specialist-accessible, introduction may be found in (33); here we follow the mathematical development of (34), but with a take-it-with-a-pinch-of-salt-formality engineer's version. We start off with the one-dimensional time-dependent Schrödinger equation given as

(16) $$\frac{d\psi}{dt} = -iH\psi.$$

Now whereas ψ —representing the wave probability distribution which, as can be seen from the right hand side of the equation— turns out to be imaginary, the term H is real and accounts for the potential and kinetic energy of the particle; reassuringly, it is referred to as the *Hamiltonian*, just like in classical mechanics. The solution for this equation (initial conditions aside) in time is just

(17) $$\psi(t) = e^{(-itH)}\psi(0);$$

which is also in the same form as that encountered in dynamical systems theory. Although the usual *physical* meaning of H is reasonably clear (it's a scalar, it's real, it's kinetic plus potential energy), it carries some mathematical baggage needed to make things work; the good news is that the same mathematical make-up is also going to make it very recognisable to practitioners in other scientific disciplines where graph Laplacians are used. In the first place the exponentiation operator $e^{(\bullet)}$ must be unitary: a way to understand this is that the dynamical system evolves in such a manner that it is bounded and conservative so that the absolute eigenvalues of the transformation are identically=1. I draw analogies with rotations on a plane, symplectic transformations or orthogonal matrices, depending on the application. In order for the time evolution to be unitary, H must be *infinitesimal stochastic*[3], which sounds very complicated but, as it turns out, simply implies that its columns must add up to zero and its off-diagonal entries be non-negative

(18) $$\sum_i H_{i,j} = 0, i \neq j \Rightarrow H_{i,j} \geq 0.$$

It must also be self-adjoint which, because it is real, implies

(19) $$H_{i,j} = H^*_{j,i} = H_{j,i},$$

[3] This is a property of a mathematical operator not a physical system.

Noting that H is time-independent and H^* implies complex conjugacy, in order to obey Eq. (19) its diagonal terms must be as follows

(20) $$H_{ii} = -\sum_{i \neq j} H_{i,j}$$

So there we have it, H, is mathematically identical to a graph Laplacian; just like for a spring-mass system. The key idea arose from the analogy of how the Laplacian drives the evolution of random walks on graphs; Fahri et al. (16) suggested that a quantum walk on a graph (at least a symmetric one) could be expressed by replacing H with the graph Laplacian.

The interest in this issue arises in the way in which quantum and random walks differ. It appears that many computational complex problems, such as scheduling, sorting, encryption, etc., rely on or are hampered by the fact that the visiting—or hitting times— based on classical search methods such as random walks may increase exponentially with the size of the network. This is exemplified by a classical random walk on a line which exhibits a Gaussian distribution in such a manner that, if we start the walk from the central node, the probability of visiting/hitting a node at the ends of the line is much smaller than visiting the nodes about the centre Figure 11. In contrast, for a quantum walk, Figure 11 and Figure 12, the peak probability is found at nodes at either end of the line (33). This is achieved by the effect of quantum entanglement which, boils down to stating that, until the quantum state is interrogated, the particle may be widely distributed over the entire network much more quickly that would be the case for a random walk.

The current interpretation for quantum dynamics dictates that when a particle leaves a node having more than one neighbour it will travel to all neighbours according to some probability distribution, and until it is measured it will be in all those neighbours (conversely, in a classical random walk a particle may end up in one, and only one, of the origin's neighbours according to a probability distribution which is also dependent on the graph Laplacian). In fact it has been proposed in (35) that for classical random walks generated by functions of the form of Eq.(21)

(21) $$S(t) = e^{(-tH_c)}; \quad H_c = LD^{-1}.$$

Whereas they suggest that for the corresponding quantum walk

(22) $$U(t) = e^{(-itH_Q)}; \quad H_Q = D^{-1/2} L D^{-1/2}$$

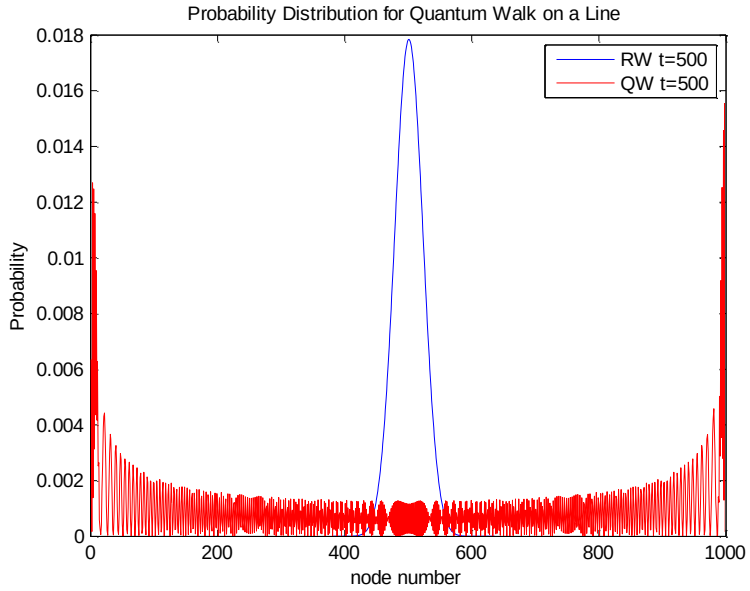

Figure 11 - Random and quantum walk probability distribution on a line at t=500 for a walk starting at the centre (node 501).

The Gaussian distribution—blue line—always accumulates and peaks at the centre and spreads slowly to the ends of the line, whereas the wave-fronts of the quantum walk—red line—has reached and peaked at the ends of the line for the same number of steps.

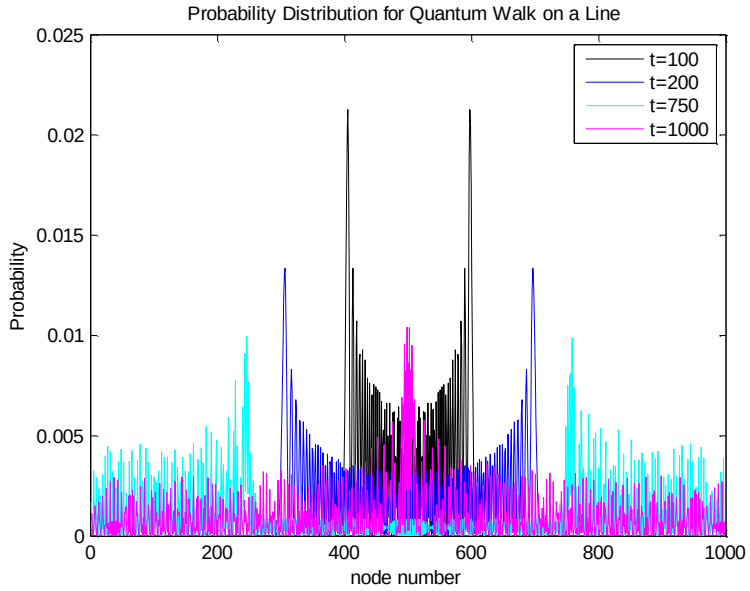

Figure 12 - Travelling quantum wave fronts on a line shown for t=100,200,750 and 1000.

The walk starts at the centre node (501) and expands out as a wave front, (black and blue in that order) eventually reaching the line ends at nodes 0 and 1000 (the red line of Figure 11 above), then bouncing back and progressing back towards the centre again (cyan shown for t=750). Eventually the two reflected wave fronts collide at the centre (magenta) at t=1000.

Upon interrogation the position of the particle is defined by the principle of quantum wave collapse and the particle is observed at a specific location—I find this analogous to a classical modal participation product where the observation vector projects all the probabilities onto one position.

The main point of this is that it is claimed that quantum walks visit graphs always as fast, but usually exponentially faster, than their classical random counterparts. But this has not been exhaustively proved yet (35).

For this reason the study of the spectral properties of graph Laplacians may play a fundamental role in the design of quantum computation and cryptography; hence the ever-increasing rise in publications in this area.

MULTIVARIATE ANALYSIS: EMPIRICAL LAPLACIANS FROM COVARIANCE MATRICES

Symmetric Laplacians and covariance matrices are particular cases of Hermitian matrices with real-valued entries. Now we will show through the spectral theorem, that for physical systems certain equivalences can be drawn between the ratios of the covariance matrices of physical parameters and the system's Laplacian.

In (36) it was shown how by evaluating the ratio of the covariances of non-linear structural processes, it was possible to determine the time-varying natural frequencies. The validation of the concept was presented in the form of a heuristic proof relying on the implicit assumption that the covariance ratios of the structural forces and deflections relate to the stiffness. Here we provide a simple but explicit proof via the extension of the concept of the stiffness matrix as a Laplacian.

Consider the results of an experiment composed of *m* samples from an *n*-degree-of-freedom system as given by two matrices $\mathbf{f}_{m,n}$ and $\mathbf{e}_{m,n}$ representing the forces and extensions respectively.

Let us consider the matrix ratio as suggested in (36)

$$\frac{\mathrm{cov}(\mathbf{f}_{m,n})^{0.5}}{\mathrm{cov}(\mathbf{e}_{m,n})^{0.5}}, \tag{23}$$

noting that the authors took the square root of the covariance assuming it has units of structural stiffness, N/m.

For an interval of measurement where it can be assumed that the system is a locally linear, equilibrium dictates that resultant force equals the extension times the stiffness:

$$\mathbf{f}_{m,n} = \mathbf{e}_{m.n} \cdot L_{n,n}, \tag{24}$$

i.e. the force matrix is a (locally) linear transformation of the extension matrix by the Laplacian stiffness $L_{n,n}$. This leads to the following expansion, where for simplicity we have dropped the algebraic indices,

$$\frac{\mathrm{cov}(\mathbf{f})^{0.5}}{\mathrm{cov}(\mathbf{e})^{0.5}} = \frac{\mathrm{cov}(\mathbf{e} \cdot L)^{0.5}}{\mathrm{cov}(\mathbf{e})^{0.5}}. \tag{25}$$

Expanding the term inside the numerator and through consideration of the spectral matrix theorem we have:

$$\frac{\mathrm{cov}(\mathbf{f})^{0.5}}{\mathrm{cov}(\mathbf{e})^{0.5}} = \left(L\right)^{0.5} \mathrm{cov}(\mathbf{e})^{0.5} \left(L'\right)^{0.5} \mathrm{cov}(\mathbf{e})^{-0.5}. \tag{26}$$

Finally, by pre and post multiplying by $L^{\pm 0.5}$ we arrive at

$$\frac{\mathrm{cov}(\mathbf{f})^{0.5}}{\mathrm{cov}(\mathbf{e})^{0.5}} = \left(L\right)^{0.5} \cdot \left(L\right)^{0.5} \overbrace{\mathrm{cov}(\mathbf{e})^{0.5} \left(L'\right)^{0.5} \mathrm{cov}(\mathbf{e})^{-0.5} \cdot \left(L\right)^{-0.5}}^{I} \tag{27}$$

And consequently

$$\frac{\mathrm{cov}(\mathbf{f})^{0.5}}{\mathrm{cov}(\mathbf{e})^{0.5}} = L. \tag{28}$$

This sketch proof says that the square root ratio of the force and displacement covariance matrices results in the full Laplacian stiffness matrix[4].

We can also express the Laplacian in spectral form by re-arranging the covariance matrix in spectral form as follows

$$L = \psi_f \lambda_f^{0.5} \psi_f' \psi_e \lambda_e^{-0.5} \psi_e'. \tag{29}$$

Concerning the pairing of the extension and force eigenstates ψ_e, ψ_f, we can draw a loose analogy with the concept of diabatic versus adiabatic process for the rate of change of the eigenstates in

[4] Here we have assumed that L is symmetric; however, as we shall show below, it is possible that $L \neq L'$, in which case the interpretation of Eq.(24) is not a trivial substitution of L for L'. The usual symmetric resultant forces from applied displacements no longer holds as the resultants are path-dependent.

quantum mechanics. If we assume that the rate of change of the force and displacement eigenstates adopt the same rate as the forcing function over the time-sampling window, we can simplify by pairing the eigenstates thus: $\psi_e = \psi_f = \psi$, so that

(30) $L = \psi \lambda_f^{0.5} \lambda_e^{-0.5} \psi'$.

However, if the rate of change between the corresponding extension and force eigenstates are not comparable they do not coincide and we must resort to Eq. (29).

AN EXAMPLE FROM COUPLED BRIDGE PIERS

We provide an example for the case of a non-linear system consisting of 15 coupled 'bridge piers'. In the first instance we compare the original force time series with that reconstructed with the global response Laplacian (i.e. that obtained using a single sampling window spanning the whole length of the time series) as shown in Figure 13. In addition we also show the modal forces and displacements using a moving time window of 100 points in Figure 14 top and bottom respectively.

Comparing the Cartesian forces directly to those obtained from the modal transformation using Eq. (24), we obtain the response shown in Figure 15 (top), and for a clearer comparison we show the response of Node 10 (bottom) which demonstrates a satisfactory agreement. Whereas in the reconstructions above a single, global, window was used, we can also generate and inspect the dynamics of the evolution of each of the 225 components of the 15x15 Laplacian for smaller overlapping time windows.

We have shown selected components from the full 225 component set in Figure 16 , wherefrom we note some interesting phenomena. In the first place we note that the Laplacian is not constant, reflecting the non-linear behaviour of the system due to yielding in the column elements. What is more interesting and merits further investigation is that the Laplacian is not always symmetric; thus for example whereas $L3,1$ and $L1,3$ are reasonably symmetric, $L14,15$ and $L15,14$ appear to be anti-symmetric. There are other numerous examples of anti-symmetry or, in some cases, little or no limited similarity. However, what is of particular interest is that whereas such matrices are clearly non-symmetric their spectra remain real-valued at all times and this is born from the fact that given that source force and displacement covariance matrices are positive semi-definite and symmetric, their eigen-properties, and hence their products, as in Eq. (29) must also be real-valued.

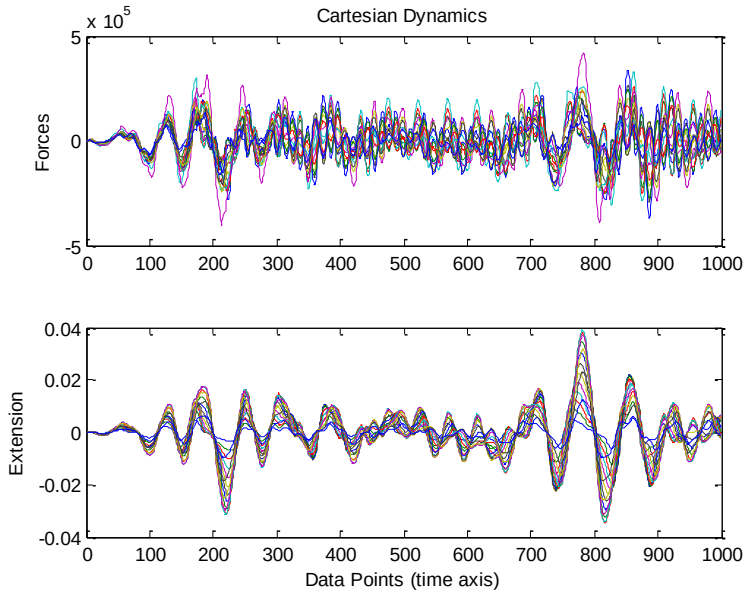

Figure 13 - Forces and displacements shown in Cartesian coordinates for 15-degree-of-freedom structural system.

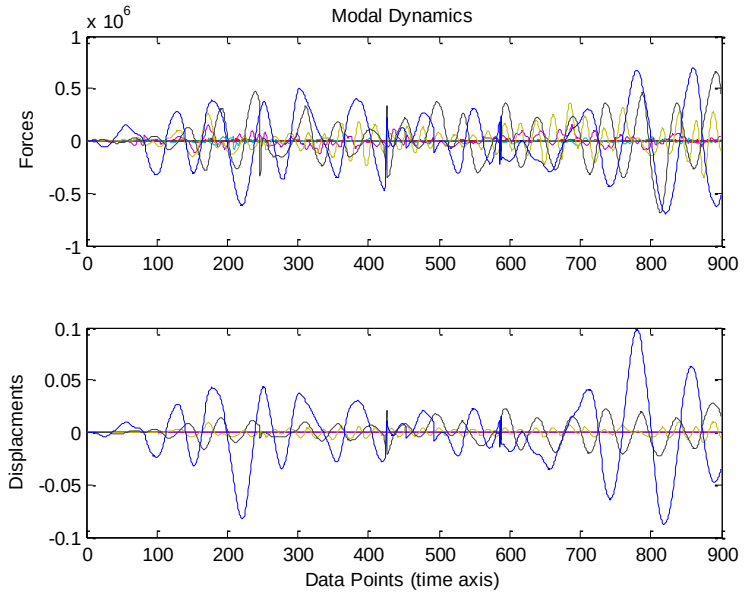

Figure 14 - Forces and displacements shown in modal coordinates with overlapping time window of 100 points.

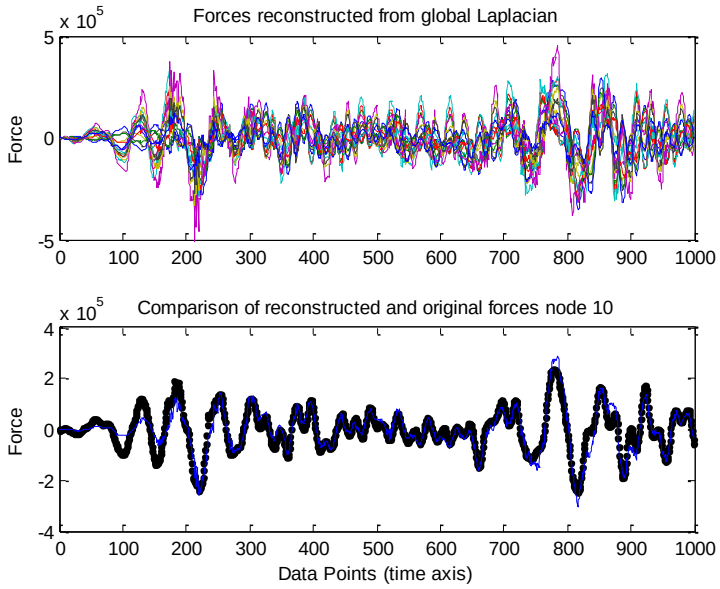

Figure 15 - Verification of reconstruction of forces in Cartesian coordinates from the global Laplacian matrix.

Even using a global Laplacian to project data in the form of Eq. (24), the reconstruction is quite successful. A detail of node 10 is shown below for both the original and reconstructed curves.

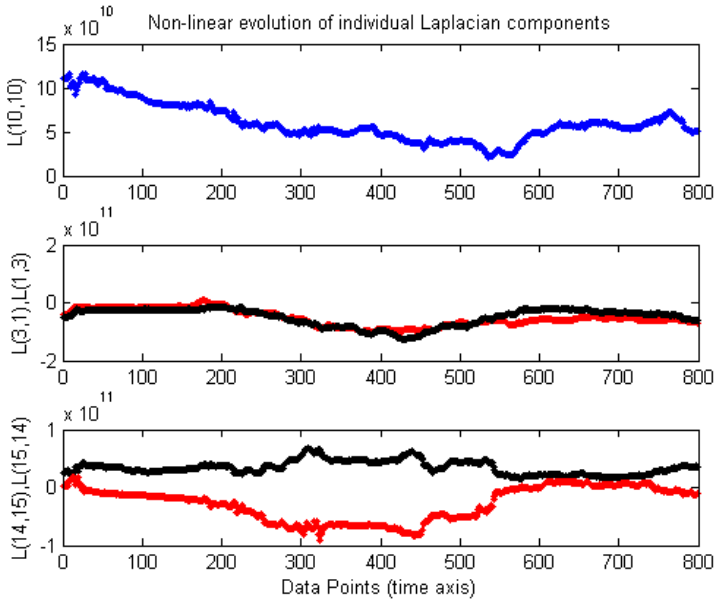

Figure 16 - The evolution of some of the 225 (15x15) components of the Laplacian (stiffness matrix).

Top: diagonal term Node 10 *L(10,10)*. Middle: Expected symmetry between Nodes 1 and 3 terms *L(3,1)* and *L(1,3)*. Bottom: apparent anti-symmetry between Nodes 14 and 15 as seem in terms *L(14,15)* and *L(15,14)*. 200 point window size.

We have sketched a proof of the equivalence between Laplacians and the covariance of the time series of a mechanical system. The sequitur is that because the time-varying Laplacian is the representation of a network's connectivity over time, then it too is a time series. So what we are looking at in Figure 16, is both a time series as well as the evolution of the individual terms of the *n*-degree Laplacian, which is also a representation of a graph.

So, to recap:

In the first instance we transformed the *m*-sampled, *n*-dimensional, time-series matrix to a graph Laplacian of degree *n* by covariance matrix ratios. We showed how we could do this either for the full length of the time series (global) or by dissecting and splicing the *m*-sampled time series into smaller blocks or windows (that may or may not overlap) so as to span the complete *m* dimension. In this sense we generated a concatenated set of graphs G^m with associated Laplacians L^m each of which represents the system within that time interval.

If the L^m change from one window to the next then, in essence, we are looking at time-varying graph (in the sense that the degree of the graph is invariant but the values of the edges $L^m_{i,j}$ change from one window to the next), thus reflecting the non-linear behaviour of the system.

The representation of time series as graphs has received much attention in the past decade or so. A number of approaches exist as there is no canonical method on how to do so ((37), (38) (39)), here we will not dwell on a comparison or exhaustive criticism of the merits of the various techniques, but we suggest that such techniques will form the basis for future analytical methods to develop an understanding of complex system behaviour.

CONCLUDING REMARKS

We have tried to show how the graph Laplacian is not an abstract combinatorial construct, but rather, a useful tool that can be used to extract meaningful knowledge from a wide variety of information sources.

We have examined how Laplacians arise in a number of fields, each with a sometimes completely unrelated application. Moreover, we have shown a number of examples and pointed to other studies that have demonstrated that the dual graph⇔time-series relationship means we can study one via the other.

Because the Laplacian plays such an important role in many physical properties, and because the spectra of graphs provides a powerful and concise way of not only quantifying but also qualifying the connectivity of graphs, then it is only logical that we follow our considerations of graph spectra in the future by exploring new applications areas in engineering systems (we are particularly interested in sensor network deployment and signal processing); however, we stress that the methods presented here can be applied to other, even, 'non-physical' systems including natural languages.

BIBLIOGRAPHY

1. **Schrödinger, E.** *What is Life?: The Physical Meaning of the Living Cell.* Cambridge : Cambridge University Press, 1944.

2. **O'Connor, T., Wong, H. Y.** Emergent Properties. *The Stanford Encyclopedia of Philosophy.* [Online] Summer 2015. [Cited: 19 7 2016.] <http://plato.stanford.edu/archives/sum2015/entries/properties-emergent/>.

3. *On the mathematics of Emergence.* **Cucker, F., Smale, S.** 2007, Japan. J. Math., Vol. 2, pp. 197-227.

4. *Self-Organized Criticality.* **Bak, P., Tang, C. and Weisenfeld K.** July 1988, Phys. Rev. A, Vol. 38, pp. 364-374.

5. **Mikhailov A.S., Calenbuhr V.** *From cells to societies: Models of Complex Coherent Action.* Berlin Heidelberg : Springer -Verlag, 2002.

6. *From Kuramoto to Crawford: exploring the onset of synchronization in populations of coupled oscillators.* **Strogatz, S.H.** 2000, Physica D, Vol. 143, pp. 1-20.

7. *Scale invariance and intermittency in a creep-slip model of earthquake faults.* **Hähner, P., Drossinos, Y.** 6, June 1999, Phys. Rev. E, Vol. 59, pp. R6231-4.

8. *The Equivalence between feedback and dissipation in impact oscillators.* **Gutiérrez, E., Arrowsmith, D.K.** 1, 2007, Int. J. Bifurcations and Chaos, Vol. 17, pp. 255-269.

9. *Ninety plus thirty years of nonlinear dynamics: Less is more and more is different.* **Holmes, P.** 9, 2005, Int. J. Bifurcations and Chaos, Vol. 15, pp. 2703-2716.

10. *Emergence of scaling in random networks.* **Barabasi, A.L., Albert, R.** 1999, Science, Vol. 286, pp. 509–511.

11. *Error and attack tolerance of complex networks.* **Albert R., Jeong H., Barabási A.L.** 2000, Nature, Vol. 406, pp. 378-382.

12. *Collective dynamics of 'small-world' networks.* **Watts, D. J., Strogatz, S. H.** 1998, Nature, Vol. 393, pp. 440–442.

13. **Abarbanel, H.D.I.** *Analalysis of observed chaotic data.* New York : Springer-Verlag, 1996.

14. *Spectral embedding of graphs.* **Luo, B., Wilson, R.C., Hancock, E.R.** 2003, Pattern Recognition, Vol. 36, pp. 2213 – 2230.

15. **Ayazifar, B.** *Graph Spectra and Modal Dynamics of Oscillatory Networks.* Massachusetts Institute of Technology. 2002. PhD Thesis.

16. *Quantum computation and decision trees.* **Farhi, E., Gutman, S.** 1998, Phys. Rev. A, Vol. 58, pp. 915-928.

17. **Chung, F.** *Spectral Graph Theory (CBMS Regional Conference Series in Mathematics).* s.l. : American Mathematical Society, 1997. Vol. 92.

18. *Laplace eigenvalues of graphs-- a survey.* **Mohar, B.** 1992, Discrete MAthematics, Vol. 109, pp. 171-183.

19. **Baltz, A, Kliemann, L.** Spectral Analysis. [ed.] U., Erlebach, T. Brandes. *Network Analysis Methodological Foundations.* Heidelberg : Springer-Verlag Berlin, 2005, pp. 373-416.

20. *The Laplacian spectrum of graphs.* **Mohar, B.** [ed.] Alavi Y., et al., et al. New York : Wiley, 1991. Proceedings of the Sixth Quadrennial International Conference on the Theory and Applications of Graphs, Western Michigan University. Vol. 2, pp. 871-898.

21. **Newman, M. W.** *The Laplacian Spectrum of Graphs.* Winnipeg : University of Manitoba, 2000. Master of Science Thesis.

22. *Laplacian Matrices of Graphs: A Survey.* **Merris, R.** 1994, Linear Algebra and Its Applications, 197,198, pp. 143-176.

23. *Algebraic Connectivity of Graphs.* **Fiedler, M.** 1973, Czech. Math. J., Vol. 98, pp. 298-305.

24. **Gutiérrez E., Caperan P., Morris S.** *A case study in vulnerability analysis of high-voltage electricity transmission systems from a sector of the European grid.* Institute for the Protection and the Security of the Citizen, Joint Reserach Centre. Ispra : European Commission, 2005. Tech. Note I.05.09.

25. *Application of modal analysis in assessing attack vulnerability of complex networks.* **Petreska, I., et al., et al.** 2009, Commun. Nonlinear Sci. Numer. Simulat., Vol. 15, pp. 1008-1018.

26. **Chopra, A.K.** *Dynamics of Structures: theory and applications to earthquake engineering.* Upper Saddle River, NJ : Prentice-Hall, 2000.

27. **Strozzi, F., Renaldi, G., Gutiérrez, E.** *Network Segmentation and Spanning Sets, JRC 99540.* IPSC, Joint Research Centre. Ispra : European Commission, 2015.

28. *Road Traffic: A case study in flow and path-dependency in weighted directed networks.* **Bono, F., Gutiérrez, E., Poljanseck, K.** 2010, Physica A, Vol. 389, pp. 5287-5297.

29. *Autocatalytic, bistable, oscillatory networks of bilogical relevant organic reactions.* **Semenov, S. et al.** 29 September 2016, Nature, Vol. 537, pp. 656-560.

30. **Helbing, D.** Traffic and related self-driven many-particle systems. *Rev. Mod. Phys.* 2001, Vol. 73, 4, pp. 1067-.

31. *Emergent Behaviour in Flocks.* **Cucker, F., Smale, S.** 5, May 2007, IEEE Trans. Autom. Control, Vol. 52, pp. 852-862.

32. **Henriques, M.** BBC Earth. *BBC.* [Online] BBC, 18 July 2016. [Cited: 1 November 2016.] http://www.bbc.com/earth/story/20160715-organisms-might-be-quantum-machines.

33. *Quantum random walks- an introductory overview.* **Kempe, J.** 4, 2003, Contemporary Physics, Vol. 44, pp. 307-327.

34. *Quantum Techniques for Stochastic Mechanics.* **Baez, J., Biamonte, J.** arXiv:1209.3632.

35. *Degree distribution in Quantum Walks on Complex Networks.* **Faccin, M., Johnson, T., Biamonte, J., Kais, S., Migdal, P.** 041007, 2013, Phys. Rev. X, Vol. 3.

36. *The application of Karhunen-Loeve, or principal component analysis method, to study the non-linear response of structures.* **Gutiérrez, E., Zaldivar J.M.** 2000, Earthquake Engng. Struct. Dyn., Vol. 29, pp. 1261-1286.

37. **Strozzi, F., Zaldivar, J.M., Poljansek, K., Bono, F., Gutiérrez, E.** *From Complex networks to time series and viceversa: Application to metabolic networks.* IPSC, Joint Research Centre. Ispra : European Commission, 2009. EUR 23947 EN.

38. *From time series to complex networks: The visibility graph.* **Lacasa, L., Luque, B., Ballesteros, F., Luque, J., Nuño J.C.** 13, 1 April 2008, PNAS, Vol. 105, pp. 4972-4975.

39. *Complex Network from Pseudoperiodic Time Series: Topology versus Dynamics.* **Zhang, J., Small, M.** 238701, 16 June 2006, Phys. Rev. Lett., Vol. 96.

40. *Isoperimetric Numbers of Graphs.* **Mohar B.** 47, 1989, J. Combinatorial Theory, Vol. B, pp. 274-291.

ACKNOWLEDGEMENT

The source data for Figure 13 to Figure 16 are generated from the results of the work by Carlo Paulotto. For more information see the publication Paulotto C, Ayala G, Taucer F, Pinto Vieira A , S*implified Models/Procedures for Estimation of Secant-to-Yielding Stiffness, Equivalent Damping, Ultimate Deformations and Shear Capacity of Bridge Piers on the Basis of Numerical Analysis*, EUR 22885 EN. Luxembourg (Luxembourg): OPOCE; 2007.

APPENDICES: SUNDRY CONCEPTS AND EQUATIONS

A. Raleigh quotient, Courant-Fischer principle and Fiedler Eigenvalue

Given a Hermitian matrix M and some an arbitrary-valued vector $x \neq \mathbf{0}$ the Raleigh quotient (18) (22) is defined as

(31) $$R(x, M) = \frac{x^* Mx}{x^* x};$$

where $x^* x$ is the inner product, and x^* represents the complex conjugate of x. For real-valued matrices and vectors M is simply symmetric and the conjugate transpose of x reduces to its transpose x'.

The Courant-Fischer principle (17) states that the smallest non-zero eigenvalue of a symmetric matrix M is given by

(32) $$\lambda_1(L) = \min_{x \perp \mathbf{1}_n} \frac{x'Mx}{x'x},$$

and where x is an eigenvector of M and **1**n is the ones vector associated with $\lambda_0 = 0$, and $\lambda_1 > 0$ is referred to in the literature as the Fiedler eigenvalue.

B. Normalised Fiedler

Let g be a function which assigns an (arbitrary) value to each vertex $v \in V$ of G (g can be an eigenvector of L). We can express the Rayleigh quotient

(33) $$\frac{g'Mg}{g'g} = \frac{\sum_{v_j \sim v_k} \left(f(v_j) - f(v_k) \right)^2}{\sum_{v_{i \in V}} f(v_i)^2 d_{v_i}}$$

where $f = g \cdot D^{-1/2}$ and D is the degree matrix of G. Then from Courant-Fischer and Raleigh quotient we have

(34) $$\lambda_1(L) = \inf_{f \perp T\mathbf{1}_n} \frac{\sum_{v_j \sim v_k} \left(f(v_j) - f(v_k) \right)^2}{\sum_{v_{i \in V}} f(v_i)^2 d_{v_i}}$$

$f = g \cdot D^{-1/2}$ and $v_j \sim v_k$ indicates adjacency of nodes v_j, v_k and

(35) $$\sum_{v_j \sim v_k} \left(f(v_j) - f(v_k) \right)^2$$

is the Dirichlet sum of G (see (17)),

C. Laplace Beltrami equivalence

The graph Laplacian is equivalent to the Laplace Beltrami operator for Riemannian (i.e. non Euclidian) surfaces (manifolds). It looks like the equation for the Fiedler expression above

(36) $$\lambda_S = \inf \frac{\int_S |\nabla f|^2}{\int_S |f|},$$

where *f* can be any function such that $\int_S f = 0$, i.e. a function whose net sum running round *S* (the 'surface') is zero

D. Alternative form of Dirichlet sum

In section C above we presented the definition of the Fiedler eigenvalue in terms of the Direchlet sum of a graph. Also in the section *Laplacians* in action above, we presented the vertex Gradient of a graph as the difference between the assigned values of adjacent vertices, which can be expressed in terms of the adjacency matrix as

(37) $$Grad = AM - (A'M)'$$

Where A is the adjacency matrix (here unweighted) and M is the diagonal matrix associated with the vertex value. Intuitively we see that the nodal gradient matrix

is defined as the signed difference between vertex values of adjacent nodes, so we can show that

(38) $$\sum_{v_j \sim v_k} \left(f\left(v_j\right) - f\left(v_k\right) \right)^2 = \tfrac{1}{2} \sum_{i \in Grad} \sum_{j \in Grad} \left(Grad_{i,j} \right)^2 = \tfrac{1}{2} \mathbf{1}' \cdot \left(Grad \right)^2 \cdot \mathbf{1}$$

where **1** is the ones vector of dimension equal to the number of vertices.

E. Isoperimetric Problems and Cheeger constants and inequalities

The interest in Isoperimetric problems (40) has been around since the ancient Greeks tried to work out geometric problems such as the shortest closed curve enclosing the most area. This leads us naturally into turning this concept on its head, so now we consider how to cut such an area into two (as equally-sized as possible) with the shortest cut.

Cheeger studied similarly motivated problems within the context of Remanian surfaces. The so-called Cheeger constants and inequalities describe certain processes (cuts and sections) on Riemann surfaces and associated these cuts to the spectral geometry. In simpler terms, Cheeger constants quantify the length of the border need to be cut in order to produce two maximal subsets of a Riemann manifold.

The Cheeeger constants and inequalities can be applied to graphs as a direct extension of Riemann manifolds. Consider a connected graph defined as above and we wish to divide the vertex set V into two arbitrary subsets S and its complement $\bar{S}$ such that $S \cup \bar{S} = V(G)$. The border edge set ∂S is the set of edges $(S, \bar{S})$; more formally

(39) $$\partial S = \left\{ (v_i, v_j) \in E(G) : v_i \in S, v_j \notin S \right\}$$

The smallest ratio of the edge set to volume of the smallest cut set is given as

(40) $$h_G(S) = \frac{\left| E(S, \bar{S}) \right|}{\min(\text{vol } S,\ \text{vol } \bar{S})}$$

Noting that there are many possible combinations of S and $\bar{S}$ in $V(G)$, the Cheeger constant, or isoperimetric number, is given as the smallest possible combination such that

(41) $$h_G = \min_S h_G(S)$$

In other words, there is a cut that minimises the number of cut edges whilst maximising the size of the smaller tomed component.

Below we show how to calculate hg for the some special cases and for a whole graph. In Figure 17 we show a connected graph whose nodes consists of circles

and triangles with the border set ∂S between triangles and circles shown as dotted lines.

If we are interested in separating triangles from circles, then the elimination of the perimeter border edge set $\partial S = \{e, f\}$ results in two connected components and one isolate

$$\text{(42)} \qquad \text{Perimetric measures} \begin{cases} S = \text{Triangles}, \bar{S} = \textit{Circles} \\ \left|E(S,\bar{S})\right| = \left|\{e,f\}\right| = 2, \\ \text{vol}S = 3, \text{vol}\bar{S} = 4 \end{cases}$$

$$\text{(43)} \qquad h_G(T,C) = \frac{2}{3}$$

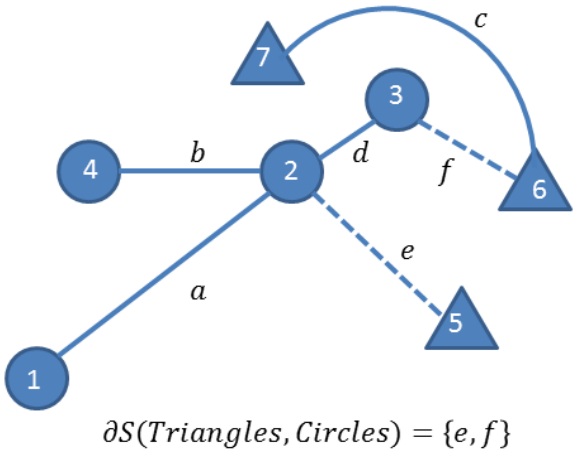

.

Figure 17 - The triangle-circle border edge set.

However, for the graph as a whole, irrespective of the vertex type, we can see that by eliminating edge d we maximize the size of the smallest group (nodes {3,6,7} two triangles and the top circle) , in which case

$$\text{(44)} \qquad h_G = \frac{1}{3}.$$

The interesting thing about the Cheeger constant is that it is associated to the Fiedler eigenvalue of the Laplacian matrix as follows (17):

$$\text{(45)} \qquad 2h_G \geq \lambda_1 \geq \frac{h_G^2}{2}$$

So we have that the Fiedler eigenvalue of the Laplacian for the TC graph is 0.295, so indeed

(46)
$$2h_G \geq \lambda_1 \geq \frac{h_G^2}{2}:$$
$$\frac{2}{3} \geq 0.295 \geq \frac{1}{18}$$

If we examine each of the components of the associated Fiedler eigenvector we note that we can group then as either negative or positively valued, noting that vertices {1 2 4 5} and {3 6 7} would form two independent connected groups by cutting link d. In essence if we cut the links between vertices of different sign we optimize the bisection; in this case only one such link exists.

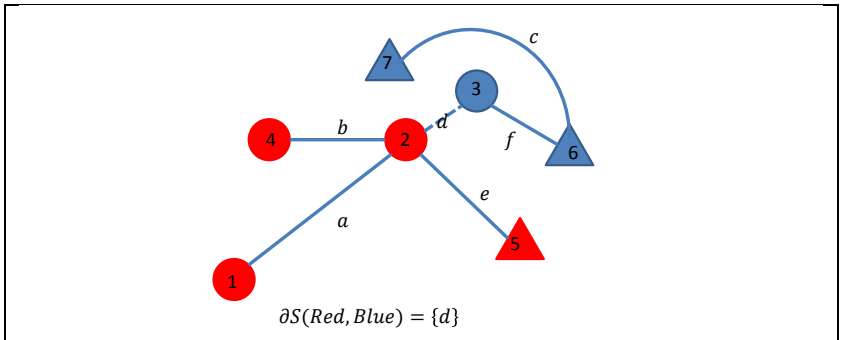

v_i	1	2	3	4	5	6	7
$\psi_{1,i}$	0.33	0.23	-0.13	0.33	0.33	-0.45	-0.64

Figure 18 - The Fiedler eigenvector $\psi_{1,i}$ and the associated vertex set v_i .

The original graph is optimally divided into two components shown as blue and red nodes. Blue (respectively red) nodes are projected with the negative (positive) eigenvector values. It can be seen that edge *d* links blue and red nodes, i.e. transitions from node 2 ($\psi_{1,2} = 0.23$) to node 3 ($\psi_{1,3} = -0.13$)

LB-NA-28191-EN-N

JRC Mission

As the science and knowledge service of the European Commission, the Joint Research Centre's mission is to support EU policies with independent evidence throughout the whole policy cycle.

EU Science Hub
ec.europa.eu/jrc

@EU_ScienceHub
EU Science Hub - Joint Research Centre
Joint Research Centre
EU Science Hub

Publications Office

doi:10.2788/1139

ISBN 978-92-79-63458-1